Lawrence Livermore National Laboratory

Energy dependence of chain fission product yields from neutron-induced fission of 235U, 238U, and 239Pu

A Ramirez, J Silano, A Tonchev

June 2025

Disclaimer

This work performed under the auspices of the U.S. Department of Energy by Lawrence Livermore National Laboratory under Contract DE-AC52-07NA27344.

Energy dependence of chain fission product yields from neutron-induced fission of ^{235}U, ^{238}U, and ^{239}Pu

(Dated: June 1, 2025)

I. CUMULATIVE FISSION-PRODUCT YIELDS

The distribution of fission product yields at the late stages of the fission process, which is governed by beta decay and delayed neutron emission, is one of the most basic quantities that has been observed since the discovery of fission. Cumulative fission product yields (CFPY) are vital to many applications, including the development of advanced reactors and transmutation systems, estimation of decay heat in nuclear reactors, radiation shielding, isotope generation and others. In large part, for these reasons, the demand for high-quality CFPY data in such applications is rapidly increasing. Cumulative and independent FPY data are currently based mainly on England and Rider's evaluation from the mid-1990s [1] and contain only three energy points: thermal (0.025 eV), fast (0.5 MeV), and high (14 MeV) incident neutron energies, leaving a significant gap of information for other energies. More recent evaluations of available CFPY data [2–5] presented compelling evidence for a possible energy dependence for some high-yield fission products from neutron-induced fission on major actinides in low-energy regions between thermal and 2 MeV. However, the data showing this energy dependence were derived from critical assemblies and fast reactors, which have rather broad energy distributions. Furthermore, there were no systematic studies of CFPY beyond the second or third chance fissions. The problem is further complicated by the fact that neither nuclear-physics models nor empirical nuclear-data models are able to fully reproduce the CFPY dependency over a wide range of fissile systems and neutron energies, although significant progress has been made in both areas recently [7, 8].

The lack of completeness and systematic studies of these CFPY over a broad energy range was the primary motivation for the LLNL-LANL-TUNL collaboration. We summarize all high-yield CFPY data obtained for ^{235}U, ^{238}U, and ^{239}Pu isotopes using quasi-monoenergetic neutron beams with incident energies ranging from 0.5 to 14.8 MeV.

A. Experimental overview

This collaboration effort was carried out at the Triangle Universities Nuclear Laboratory (TUNL) using a 10 MV FN tandem Van de Graaff accelerator. The method of measuring CFPY at TUNL involves three well-established approaches: (i) quasi-monoenergetic neutron beams tunable in a broad range of MeV neutrons, (ii) dual-fission ionization chambers measuring the total number of fissions during irradiation, and (iii) direct γ-ray spectroscopy with variable irradiation, decay, and measurement times. Fig. 1 illustrates a schematic of the experimental setup showing the three stages of the CFPY measurement.

First, high fluxes of fast monoenergetic neutrons between 0.5 and 14.8 MeV were produced utilizing the four charged-particle reactions ^{7}Li$(p,n)^{7}$Be, ^{3}H$(p,n)^{3}$He, ^{2}H$(d,n)^{3}$He, and ^{3}H$(d,n)^{4}$He. These reactions cover different energy ranges in which the produced neutrons are truly monoenergetic and the contribution from off-energy neutrons are negligible. Extensive effort was made in the early stages of this campaign to characterize the neutron beam conditions by performing different time-of-flight and activation measurements [9].

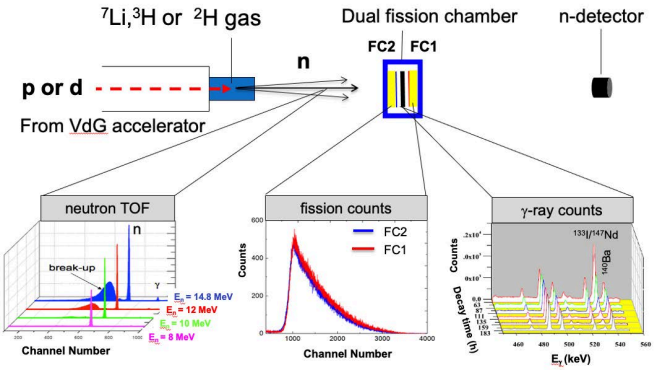

FIG. 1. (color online) Schematic of the FPY experimental setup at TUNL. The bottom left panel shows the measured neutron time-of-flight spectra, the bottom middle panel shows the fission chamber pulse-height spectra, and the right panel shows the time evolution of the γ-ray spectra after irradiation.

Second, a dual-fission chamber (DFC) chamber was used to provide the most accurate determination of the total number of fissions during the irradiation [10]. The DFC is located in close proximity (4 cm) to the neutron production source containing two thin (10-100 μg cm^{-2}) reference foils and a thicker ($\sim$200 mg cm^{-2}) actinide activation target. The activation target is contained in the center of the chamber while the thin reference foils are 4 mm up- and down-stream from the activation target. The thick activation target is composed of the same actinide

material as the thin reference foils in the adjacent chambers. The average neutron flux at the center of the DFC was measured to be 2.10^6 to 5.10^7 n $s^{-1}cm^{-2}$. Three DFCs containing highly-enriched ^{239}Pu, ^{235}U, and depleted ^{238}U, were dedicated to the three target isotopes. The advantage of using the DFC method compared to other methods such as radiochemistry, the ratio method, or mass separation, is that the total number of fissions during the irradiation can be determined without having to explicitly know either the neutron-induced fission cross section or the neutron flux. Only the ratio of the masses of the thin reference foils to the thick activation target must be known, thus greatly reducing the total uncertainty of the measurements [11].

Third, following neutron irradiation, high-resolution γ-ray spectroscopy was performed directly on the irradiated samples by taking sequential γ-ray spectra. Each fission product was identified by its γ-ray energy and its decay time to ensure that its γ-ray line was free of interference. This also allowed us to optimize the counting time for each γ-ray peak based on the half-life and the signal-to-background ratio, providing the lowest possible detection limit and minimizing uncertainty in the determination of CFPYs. One of the drawbacks of this technique is that the γ-ray spectra are quite complex, resulting in potential interference, and limiting the number of isotopes that can be identified.

In order to selectively access different CFPY along the isobaric chain, three different irradiation times were applied. Long irradiation (∼5 days) reveals the last or longest-lived (days or weeks) radioactive member of the β-decay chain [9, 12]. Short irradiation of 2-8 hours is used to target isotopes whose half-lives range from a few minutes to several hours [13]. These fission products are located usually 2-3 precursors away from the line of stability. Cycle activation is used to gain access to very short-lived CFPY (sub-second to five minutes) [14, 15]. These fission products are located usually 4-5 precursors away from the last stable isotope. A short summary of some of the main results will be presented in the following section.

B. Results

During the past10 years, the LLNL-LANL-TUNL collaboration performed several measurement campaigns to determine the energy evolution of various long-lived fission products from neutron-induced fission of ^{235}U, ^{238}U, and ^{239}Pu. Since they are situated at the end of a β^- decay chain, some of them can be considered to be chain yields. The summary of the main experimental results of this study have been recently published for eleven incident neutron energies of E_n=0.58, 1.37, 2.37, 3.6, 4.6, 5.5, 6.5, 7.5, 8.9, 11.0 and 14.8 MeV [16]. For each incident energy, approximately 18 cumulative FPYs were determined, nearly all being high-yield fission products, i.e., those occurring in the peaks of the fission mass distributions. The experimental results for 16 high-yield fission products are illustrated in Fig. 2, while all CFPY values are listed in the aforemention reference. Note that fission products depicted in the left two columns belong to the left mass asymmetric peak distribution (except ^{127}Sb), while the fission products in the last two columns are situated at the right mass asymmetric peak distribution.

First it is important to note that the CFPY depend on the target nucleus and neutron energy, and the scale of the energy dependance is different for different CFPY. The high precision (3-5%) of the CFPY measurements reveals an anomalous energy dependency for many of these high-yield fission products. One particular energy region is from 0.5 to about 5 MeV, where the CFPY from ^{239}Pu(n,f) and ^{238}U(n,f) have a positive slope (the yields of these isotopes increase with neutron energy). The strongest overall energy dependence was observed for ^{239}Pu(n,f). For example, the CFPY of ^{91}Sr, ^{92}Sr, ^{95}Zr, ^{97}Zr, ^{99}Mo, ^{132}Te, ^{140}Ba, ^{143}Ce, and ^{147}Nd shows a positive energy trend for E_n<5 MeV. This trend is almost linear up to about 4 MeV, confirming the earlier assessment from critical assembly measurements for some CFPY as ^{147}Nd below E_n=2 MeV [2, 5].

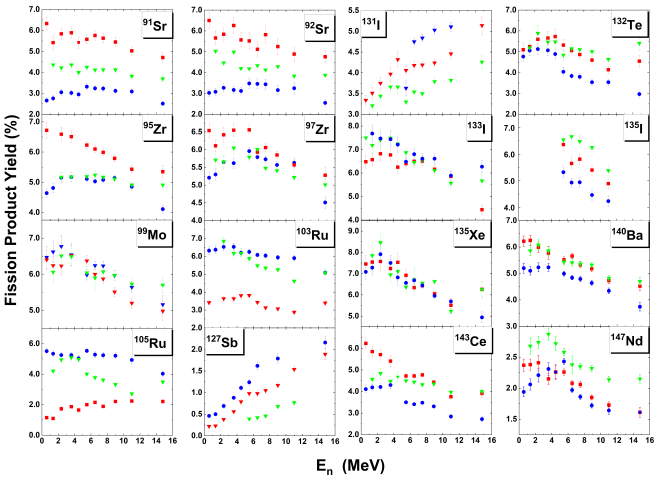

FIG. 2. (color online) Fission product yields of ^{91}Sr, ^{92}Sr, ^{95}Zr, ^{97}Zr, ^{99}Mo, ^{103}Ru, ^{105}Ru, ^{127}Sb, ^{131}I, ^{132}Te, ^{133}I, ^{135}Xe, ^{140}Ba, ^{143}Ce, and ^{147}Nd from neutron-induced fission of ^{235}U (red squares), ^{238}U (green triangles), and ^{239}Pu (blue circles). The vertical error bars represent the total uncertainties.

Contrary to this, the CFPY of ^{235}U(n,f) show a constant or slightly negative slope from 0.5 to 5 MeV. There are a few cases which do not follow these trends - specifically ^{127}Sb and ^{131}I. The CFPY of ^{127}Sb and ^{131}I steadily increase with incident energy since they are located on the steep rising slope of the right peak of the asymmetric mass distribution. The only common feature of all three actinide isotopes is the decrease of the CFPY for the asymmetric fission modes with higher incident neutron energy E_n>5 MeV, and that the decline is continuous for all fission yields towards 14.8 MeV. This is the region between the second- (E_n∼6.5 MeV) and third-chance fis-

sion (E_n∼12 MeV). These features are consistent with the global tendency suggested by the Brosa's classic fission model, while in the valley region the fission yields progressively increase as the neutron incident energies rise.

Currently, there are ongoing theoretical efforts based on macroscopic–microscopic and phenomenological frameworks to shed light on this intriguing low-energy (0.5 to 5 MeV) dependence. A calculation that included shell structure in the two asymmetric mass regions was able to reproduce the energy-dependent trend of certain CFPY from ^{235}U(n, f) [19]. For example, as can be seen from the TUNL data shown in Fig. 2, ^{95}Zr exhibits a steeper increase than ^{97}Zr, while ^{99}Mo remains nearly unchanged. This implies that isotopes closer to the doubly magic configuration N = Z = 50 are less sensitive to incident neutron energy. Additionally, ^{103}Ru and ^{105}Ru CFPY start to display an increasing trend with incident energy. Similar, heavy fission products such as ^{132}Te or ^{131}I, which are close to the double shell closure, maintain a nearly flat slope. The challenge is that this dependency is almost opposite to the CFPY from ^{239}Pu(n, f). Therefore, one should also consider the location of individual fission products in relation to the main asymmetric (the so-called S1 and S2) modes of fission, in addition to shell and pairing effects.

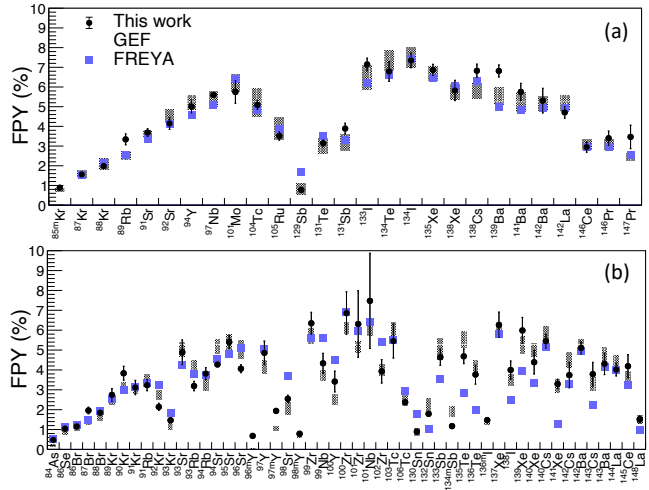

FIG. 3. (color online) Comparison of the TUNL CFPY for the ^{238}U(n, f) reaction at E$_n$= 4.6 MeV (solid points) using the Jackrabbit (a) and RABITTS (b) techniques with calculated yields from GEF [17] (green bands) and FREYA (blue bands) [18] codes.

As mentioned earlier, short irradiations were performed in order to access the region of short-lived fission products (few seconds to minutes to hours) which were over saturated during long irradiations. In these cases the so called Jackrabbit and RABITTS techniques [13, 15] were employed. The Jackrabbit technique uses the same standard procedure as discussed above, except that the irradiation time is limited to a few hours. The RABITTS (RApid Belt-driven Irradiated Target Transfer System) allows cyclic activation analysis where the target is repeatedly irradiated by the neutron beam and then counted by γ-ray detectors. The system utilizes a stepping motor and belt-driven mechanism for transporting the target between irradiation and counting positions (8 m in distance) in under 1 second with extreme stability and excellent repeatability [14]. Cyclic activation was carried out with three different cycle times to optimize the FPY measurement for various half-lives from a few seconds to minutes. Both Jackrabbit and RABITTS techniques were employed for most of the same incident neutron energies as for the long irradiation technique.

The CFPY measured using the Jackrabbit technique for the ^{238}U(n, f) reaction at E$_n$= 4.6 MeV are shown in Fig. 3 (a), while the RABITTS results are shown in Fig. 3 (b). A comparison of measured cumulative yields at TUNL and those calculated from theoretical models using the GEF [17] and FREYA [18] codes are shown in Fig. 3. The LLNL-LANL-TUNL collaboration collected a large amount of short-lived CFPY data for multiple neutron energies, but the analysis is still underway. These data will bridge the long-lived CFPY described earlier, providing self-consistent, high-precision, and time-dependent CFPY data for ^{235}U, ^{238}U, and ^{239}Pu isotopes.

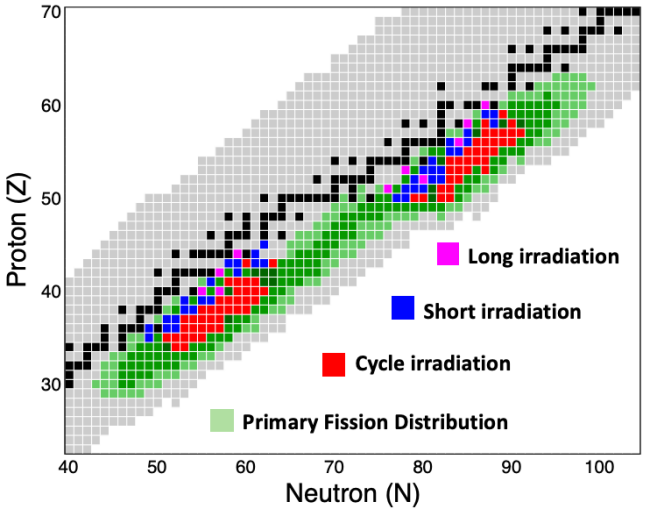

FIG. 4. (color online) Experimentally measured FPYs at TUNL using three type of irradiations: long irradiation (cyan squares), short (Jackrabbit) irradiation (blue squares), and cyclic (RABITTS) techniques (red squares) . The green squares are the independent fission-yield distribution while the black squares indicate the stable isotopes. Independent fission yields generally comprise nuclides one to six nuclear charges from stability.

II. SUMMARY

A summary of the fission isotopes for which CFPY have been measured at TUNL by all three techniques with respect to the primary fission yield distribution is shown

in Fig. 4. These measurements comprise more than 60 unique radionuclides per energy per fissioning isotope of the fission landscape spanning one to five nuclear charges away from the β-stability line. This work covers the energy range of 0.5 to 14.8 MeV with small steps in neutron energy.

For some fission products, the CFPY data indicate anomalous energy dependences below 5 MeV incident neutron energy. Since the turnaround for these high-yield fission products occurs at neutron energies of around 4 - 5 MeV, this phenomenon is more likely driven by structure effects (both paring and shell effect) than by the second-chance fission barrier, which becomes active around 6.5 MeV. There is also no visible change in the slope of these CFPYs toward higher energies, which might be affected by third-chance fission around 11 MeV. That might indicate that the mass distributions resulting from multi-chance fission are not much different from those resulting from first-chance fission. According to the present results, the CFPY is dependent on the target nucleus and neutron energy and the scale probably depends on the shell structure of the fragments as well as the location of individual fission products with respect to their main modes of fission. For many applications, the energy dependence of the CFPY distribution is crucial in order to improve the accuracy of system modeling.

III. ACKNOWLEDGMENTS

This work was supported by the US Department of Energy through Lawrence Livermore National Laboratory under contract DE-AC52-07NA27344

IV. REFERENCES

[1] T.R. England, B.F. Rider (1994), "Evaluation and compilation of fission product yields," Los Alamos National Laboratory, LA-UR94-3106.

[2] M.B. Chadwick *et al.*, "Fission Product Yields from Fission Spectrum n+^{239}Pu for ENDF/B-VII.1," Nuclear Data Sheets **111**, 2923 (2010).

[3] H. D. Selby *et al.*, "Fission Product Data Measured at Los Alamos for Fission Spectrum and Thermal Neutrons on ^{239}Pu, ^{235}U, ^{238}U," Nucl. Data Sheets, **111**, 2891 (2010).

[4] J. Laurec *et al.*, "Fission Product Yields of ^{233}U, ^{235}U, ^{238}U and ^{239}Pu in Fields of Thermal Neutrons, Fission Neutrons and 14.7-MeV Neutrons," Nucl. Data Sheets, **111**, 2965 (2010).

[5] I.J. Thompson, *et al.*, "Evaluations of Fission Chain Yields for ^{239}Pu from Fission-Spectrum Neutrons," Nuclear Science and Engineering **171**, 85 (2012).

[6] B.D. Pierson, A.M. Prinke, L.R. Greenwood, S.C. Stave, R.S. Wittman, J.G. Burch, J.T. Burke, S.W. Padgett, J.J. Ressler, G. Slavik, A. Tamashiro, A.P. Tonchev, and W. Younes, "Improved Cumulative Fission Yield Measurements with Fission Spectrum Neutrons on 235U," Nucl. Data Sheets, **155**, 86 (2019).

[7] A.E. Lovell, *et al.*, Phys. Rev. C **103**, 014615 (2021).

[8] N. Schunck, M. Verriere, G. Potel Aguilar, R.C. Malone, J.A. Silano, A.P.D. Ramirez, and A.P. Tonchev, "Microscopic calculation of fission product yields for odd-mass nuclei," Phys. Rev. C 107, **107**, 044312 (2023).

[9] M.E. Gooden, B. Fallin, C.R. Howell, J.H. Kelley, W. Tornow, C.W. Arnold, E.M. Bond, T.A. Bredeweg, M.M. Fowler, W.A. Moody, R.S. Rundberg, G. Rusev, D.J. Vieira, J.B. Wilhelmy, J.A. Becker, R. Macri, C. Ryan, S.A. Sheets, M.A. Stoyer, and A. P. Tonchev, "Energy Dependence of Fission Product Yields from ^{235}U , ^{238}U and ^{239}Pu for Incident Neutron Energies Between 0.5 and 14.8 MeV," Nuclear Data Sheets **131**, 319 (2016).

[10] C. Bhatia *et al.*, "Dual-Fission Chamber and Neutron Beam Characterization for Fission Product Yield Measurements Using Monoenergetic Neutrons," Nucl. Instrum. Methods Phys. Res. A **757**, 7 (2014).

[11] J.A. Silano, R.C. Malone, S.W. Finch, M.E. Gooden, C.R. Howell, A.P.D. Ramirez, K. Thomas, A.P. Tonchev, W. Tornow, J.B. Wilhelmy, "Characterization of ^{235}U, ^{238}U and ^{239}Pu fission ionization chamber foils by α and γ-ray spectrometry," Nucl. Instrum. Methods Phys. Res. A **1063**, 169234 (2024).

[12] M.E. Gooden, R.C. Malone, T.A. Bredeweg, E.M. Bond, S.W. Finch, C.R. Howell, Krishichayan, A.P.D. Ramirez, J.A. Silano, M.A. Stoyer, A.P. Tonchev, D.J. Vieira, and J.B. Wilhelmy, and W. Tornow, "Energy dependence of fission product yields in the second-chance fission region," Phys. Rev. C **109**, 044604 (2024).

[13] A.P. Tonchev, S.W. Finch, M.E. Gooden, C. Hagmann, C.R. Howell, Krishichayan, A.P.D. Ramirez, J.A. Silano, M.A. Stoyer, W. Tornow, A.P. Tonchev, J.B. Wilhelmy, "Toward short-lived and energy-dependent fission product yields from neutron-induced fission," EPJ Web of Conferences **239**, 03001 (2020).

[14] S.W. Finch, M.E. Gooden, C. Hagmann, C.R. Howell, Krishichayan, A.P.D. Ramirez, J.A. Silano, M.A. Stoyer, W. Tornow, A.P. Tonchev, J.B. Wilhelmy, "Development of a rapid-transit system for precision nuclear physics measurements," Nucl. Instrum. Methods Phys. Res. A **1025**, 166127 (2022).

[15] A.P.D. Ramirez, J.A. Silano, R.C. Malone, M.A. Stoyer, A.P. Tonchev, M.E. Gooden, J.B. Wilhelmy, S.W. Finch, C.R. Howell, Krishichayan, and W. Tornow, "Fission product yields from the 238U(n, f) reaction at En = 4.6 MeV," Phys. Rev. C **107**, 054608 (2023).

[16] A.P. Tonchev, J.A. Silano, A.P.D. Ramirez, R.C. Malone, M.A. Stoyer, M.E. Gooden, T.A. Bredeweg, D.J. Vieira, J.B. Wilhelmy, S.W. Finch, C.R. Howell, and W. Tornow, "Energy dependence of chain fission product yields from neutron-induced fission of ^{235}U, ^{238}U, and ^{239}Pu," Nuclear Data Sheets **202**, 12 (2025).

[17] K.-H. Schmidt, B. Jurado, C. Amouroux, and C. Schmitt, "General Description of Fission Observables: GEF Model Code," Nuclear Data Sheets **131**, 107 (2016).

[18] R. Vogt and J. Randrup, "Detailed Modeling of Fission with FREYA," Nucl. Instrum. Methods Phys. Res. A, **954**, 161225 (2020).

[19] J. Chen, Y. Mukobara, K. Fujio, S. Chiba, T. Katabuchi and C. Ishizuka, "Physics-Embedded Bayesian Neural Network (PE-BNN) to predict Energy Dependence of Fission Product Yields with Fine Structures," arxiv.org/abs/2504.17275v1, **xxx**, xxx (2025).